Electronic Supplementary Material (ESI) for Physical Chemistry Chemical Physics

Supporting Information

Spectroscopic selection of distance measurements in a protein dimer with mixed nitroxide and Gd^{3+} spin labels

Ilia Kaminker, Hiromasa Yagi, Thomas Huber, Akiva Feintuch, Gottfried Otting, and Daniella Goldfarb

Sample preparation

The mutant S114C/C157S of ERp29 was prepared as described previously.[1] The ligations of Gd^{3+} loaded C1 tag and MTSL (S-(2,2,5,5-tetramethyl-2,5-dihydro-1H-pyrrol-3-yl)methyl methanesulfonothioate) to ERp29 S114C/C157S followed previously published protocols.[1–3] The mixture of ERp29 with nitroxide and Gd^{3+} tag was prepared by mixing equal amounts of 0.1 mM solutions of the ERp29 double-mutant (henceforth simply referred to as ERp29) in 20 mM MES buffer (pD 4.9) in 80% D_2O/20% glycerol-d_8.

Spectroscopic measurements

Continuous wave EPR spectra were measured at X-band on a Bruker Elexsys 500 spectrometer. The DEER measurements were carried out on a home build spectrometer.[4,5] The Gd^{3+}-Gd^{3+} distance measurements were performed with a new setup in which the MW is transferred from the bridge to the sample with quasioptical components and corrugated waveguides designed and manufactured by Thomas Keating Ltd. Details of this setup will be described elsewhere.

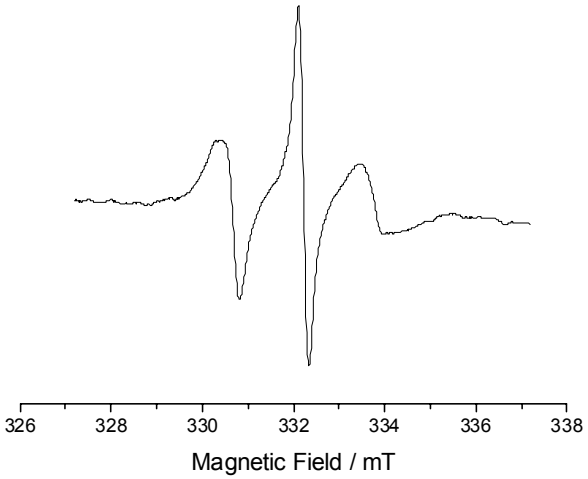

Figure S1. The room temperature continuous wave (CW) X-band EPR spectrum of the mixed labeled ERp29 sample. Parameters: modulation amplitude 0.1 mT, time constant 655 ms, MW power 50 mW. The spectrum is characteristic of a nitroxide with mild restrictions to its motion.

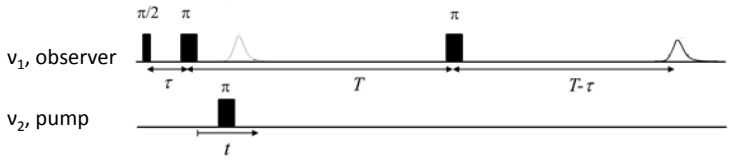

Figure S2. The four-pulse double electron-electron resonance (DEER) sequence used in the present work.[6]

Background subtraction for the Gd^{3+}-nitroxide DEER dataset

The CW EPR spectrum (Figure S1) shows that the nitroxide spin label is relatively unrestricted in its motions, suggesting that, in frozen solution, it samples many different orientations relative to the protein. We chose the pump frequency to be at the maximum of the nitroxide spectrum. At this field position the largest number of spins and orientations contribute to the echo. We expect that this, together with the motional flexibility of the spin label, should minimize orientation selection effects and we neglected them. The raw Gd^{3+}-nitroxide DEER data are shown in Figure S3a (the same dataset after background subtraction is shown in Figure 2a in the main text). Since the dipolar evolution time allowed observation of only part of the first dipolar modulation, the background decay could not be unambiguously determined in this experiment. Therefore we also acquired DEER data up to 6.3 μs, however with significantly reduced S/N ratio (Figure S3b). The sensitivity of this particular measurement was not suitable for a reliable determination of the distance distribution but allowed a more accurate determination of the background in the DEER measurement performed with shorter dipolar evolution time under otherwise identical experimental conditions. It is evident from Figure S3b that the background decay was very small. This can be attributed to the small effective sample concentration (~0.05 mM) and the pump pulse that corresponded to only a 130° rotation for the pumped spins, which reduces the modulation depth and the background decay. The background determined from the 6.3 μs measurement was used to correct the 4.3 μs dataset.

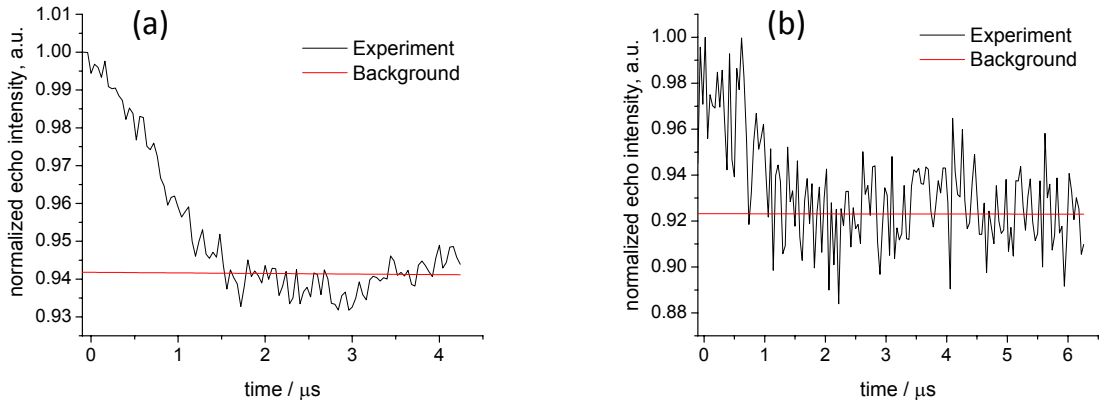

Figure S3. Raw data of Gd^{3+}-nitroxide DEER experiments. (a) Data acquired up to 4.3 µs. These data were used for determining the distance distribution. (b) Data acquired up to 6.3 µs. These data were used for determination of the background. The red lines mark the background decay used (both have the same slope).

Data analysis for the nitroxide-nitroxide DEER measurements

Two nitroxide-nitroxide DEER measurements were performed to assess possible orientation selection effects. The measurements were carried out at two observer frequencies with $\Delta\nu$ = ±65 MHz relative to the pump frequency. The two time domain traces are shown in Figure S4a before and S4b after background subtraction. The modulations are clear in both traces. The distance distributions obtained from the two traces are similar but not identical, with maxima at 5.48 nm and 5.68 nm for the experiment with $\Delta\nu$ = +65 MHz and $\Delta\nu$ = -65 MHz, respectively (Figure S4c). This small difference may be a consequence of some small orientation selection effect or of the relatively high noise level of the $\Delta\nu$ = +65 MHz trace. Also the small peaks at ~4 nm are attributed to artifacts of the distance distribution reconstruction procedure arising from the presence of noise. The low concentration of dimers with two nitroxide spin labels (~25 µM) and the long dipolar evolution time, 6.5 µs, adversely affected the S/N. Therefore, we were unable to collect DEER datasets at the g_{zz} position of the nitroxide spectrum where the EPR signal intensity is low.

As evident from the X-band CW EPR spectrum shown in Figure S1, the nitroxide spin label experienced relatively large motional freedom, this suggests that upon freezing orientation selection effects would be small. Assuming that the two measurements sampled most of the possible orientations, we combined the two DEER traces to obtain a consensus distance distribution. The resulting distance distribution is shown in Figure S4c. This distance distribution was used for the comparison with the results from molecular modeling as described in the main text.

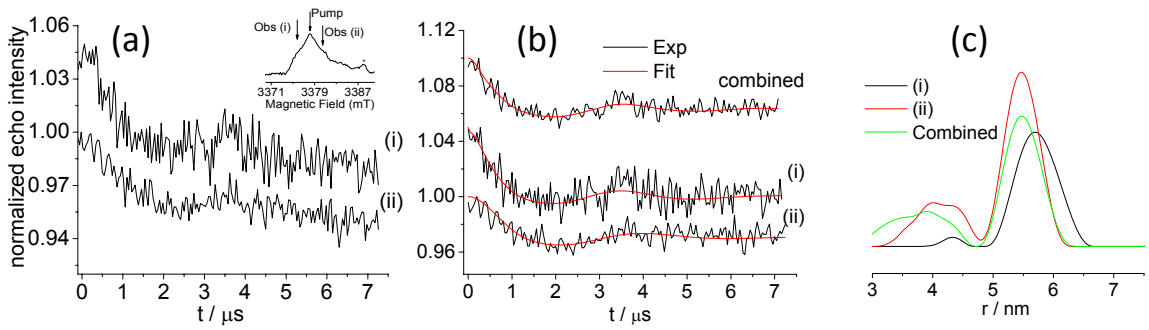

Figure S4. Nitroxide-nitroxide DEER measurements. (a) Raw DEER data. (b) DEER data after background subtraction. The combined DEER trace is the sum of the traces marked (i) and (ii). (c) The corresponding distance distributions obtained by Tikhonov regularization (regularization parameter $\alpha = 1000$) using the DEERanalysis software[7]. Experimental parameters: pump pulse of 30 ns applied at the ν_{pump} frequency (the maximum of the nitroxide spectrum); observer pulses of 50-55 (100-110) ns for $\pi/2$ (π) pulses with ν_{obs} - ν_{pump} = ±65 MHz with MW power optimized for the nitroxide spins. The trace (i) and the sum trace are displaced vertically by 0.05 units for easier comparison.

Gd^{3+} - Gd^{3+} DEER measurements

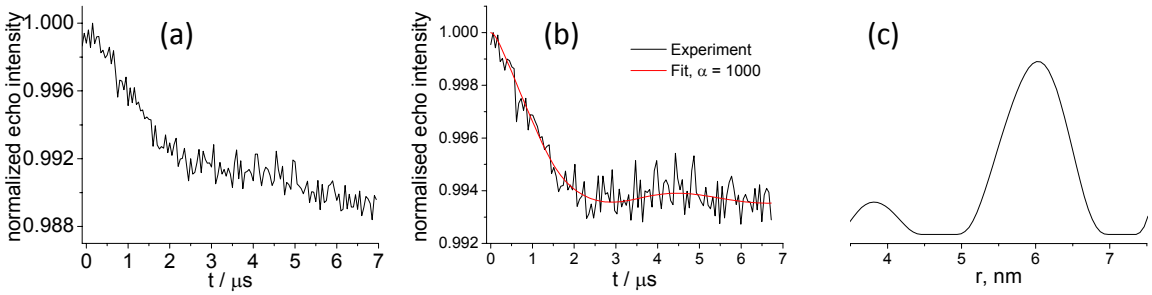

Figure S5. DEER time domain traces for the Gd^{3+}-Gd^{3+} distance measurements. Experimental parameters: T = 10 K, repetition time 200 µs, $\Delta\nu$ = 65 MHz, t_p = 15 ns, $t_{o,\pi/2}$ = 30, and $t_{o,\pi}$ = 60 ns. (a) Raw data. (b) Data after background subtraction. (c) Corresponding distance distribution.

Pump pulse off-resonance effects on the observer echo

It has been shown that the pump pulse in the DEER sequence[8,9] can have direct off-resonance effects on the observer spins, resulting in phase shifts and reduced echo amplitudes.[10] Under the conditions normally encountered in DEER experiments, this effect is limited to a phase shift of the observed echo. It does not depend on the timing of the pump pulse relative to the observer pulses in the DEER sequence and therefore can easily be corrected when the DEER experiment is set up. In the nitroxide-Gd^{3+} case, the pump pulse is applied to S = 1/2 spins while the observer spins are from the S = 7/2 spins that have a much higher transition probability than the S = 1/2 spins. Consequently, the pump pulse produces a much stronger off-resonance effect as compared to the cases where both pump and observer spins have the same spin multiplicity.

For quantitative evaluation of the influence of the pump pulse on the observer echo, we performed a set of experiments with the 3-pulse DEER sequence $\pi/2_{obs} - T - t_{pump} - (T-\tau) - \pi_{obs} - \tau -$ echo.[8,9] The experiment was performed on a Gd^{3+}-DOTA solution (0.1 mM). The magnetic field positions selected by the MW frequencies and the MW powers for the pump and observer pulses were the same as in the Gd^{3+}-nitroxide 4-pulse DEER experiment used otherwise (Figure S2). In this case, a pump pulse with a flip angle of π for the nitroxide spins corresponds approximately to a 4π pulse for the Gd^{3+} spins due to higher transition probability of the latter. We monitored the intensity of the echo as a function of the pulse length t_{pump} for three different $\Delta\nu = \nu_{pump} - \nu_{obs}$ values. Because our spectrometer does not have quadrature detection, a complex dataset was acquired by combining two datasets that had been collected separately with the reference phase set to observe the magnetization along the +x and +y direction, respectively. The echoes acquired for $\Delta\nu$ = 65 MHz along the +x direction are shown in Figure S7a. The echoes obtained after phase correction are displayed in Figure S7b. For example, a 40 ns pump pulse resulted in an echo reduction by 97% for $\Delta\nu$ = 65 MHz.

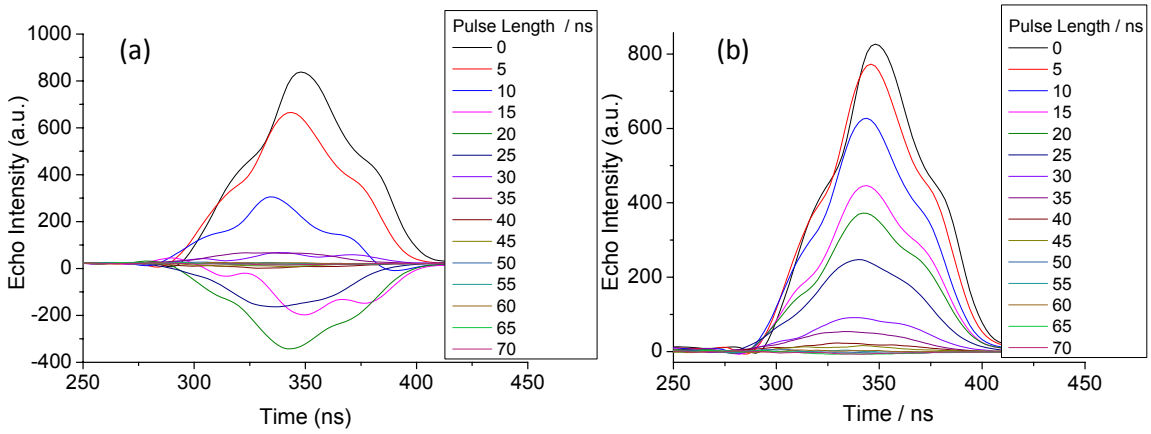

Figure S6. Hahn echo acquired along the +x direction (a) before and (b) after phase correction as a function of the pump pulse length in the 3-pulse DEER sequence. The pulse lengths at the observer frequency were 30 ns and 60 ns for $\pi/2$ and π pulses, respectively. T = 450 ns, τ = 200 ns, repetition time = 1 ms, temperature = 10 K. The phase correction angles were different for each trace in (b). The values are given in *Figure S1*.

For a theoretical description of the effect, we use the formalism introduced by Maryasov *et al.*[10] In the rotating frame of the pump frequency, the ratio of the magnetization with and without pump pulse in the three-pulse DEER sequence, $M_{Rel,}$ is given by

$$M_{Rel} = \int_{\omega_1'}^{\omega_1''}\int_{\delta'}^{\delta''}\left(A\cdot e^{-it_p(\Delta\nu+\delta)} + \frac{B-C}{2}\cdot e^{-it_p(\Delta\nu+\delta+\Omega_{eff})} + \frac{B+C}{2}\cdot e^{-it_p(\Delta\nu+\delta-\Omega_{eff})}\right) d\omega_1 d\delta \qquad (1)$$

where

$$A = \frac{\omega_1^2}{2\Omega_{eff}}; \quad B = 1 - A; \quad C = \frac{\Delta\nu+\delta}{\Omega_{eff}} \qquad (2)$$

$$\Omega_{eff} = \left|\omega_{1(S,m_s)}\cos(\beta), \omega_{1(S,m_s)}\sin(\beta), \Delta+\delta\right| = \sqrt{\omega_{1(S,m_s)}^2 + \Delta^2 + \delta^2} \qquad (3)$$

$\Delta\nu$ is the difference between observer and pump frequencies, δ is the offset of a spin packet from the observer frequency, t_p is the length of the pump pulse, β is the phase angle between the observer and pump frequencies. The transition probability for the $|S,m_s\rangle \rightarrow |S,m_{s+1}\rangle$ transition is given by $P_{S,m_S} = S(S+1) - m_S(m_S+1)$. The transition probability is different for each of the different Gd^{3+} transitions, which results in different effective MW field strengths $\omega_{1(S,m_S)} = \gamma\sqrt{P_{S,m_S}}B_1$ where B_1 is the intensity of the rotating magnetic field generated by the pump pulse, and γ is the electron gyromagnetic ratio. To account for the excitation bandwidth of the observer pulses, we took a range of offset values and integrated over this range δ'=-15 MHz, δ''=15 MHz.

For the maximum MW power we get for the nitroxide radical $\omega_{1(\frac{1}{2},-\frac{1}{2})}$ ~22.5 MHz and for different transitions of Gd^{3+} we obtain $\omega_{1(\frac{7}{2},-\frac{3}{2})}$ = 90 MHz, $\omega_{1(\frac{7}{2},-\frac{5}{2})}$ = 76.5 MHz, and $\omega_{1(\frac{7}{2},-\frac{7}{2})}$ = 58.5 MHz. We therefore used a range of ω_1 values between ω_1'=55 MHz and ω_1'' = 95 MHz with equal probability in our calculations (eq. 1) to account both for the experimental ω_1 inhomogeneity and for the fact that the observer pulses in our configuration at low temperature mostly affect spins that belong to the lower three EPR transitions (-7/2→-5/2, -5/2→-3/2, -3/2→-1/2) that form the broad background of the Gd^{3+} EPR spectrum.

Figure S7a compares the experimental echo intensities with the echo intensities calculated with eq. 1 as a function of the pulse length. The comparison of experimental versus calculated phase shifts is shown in Figure S7b. It is evident that the calculated echo intensities are in good agreement with the experiment. We therefore conclude that this simple

explanation accounts for most of the echo reduction effect without having to invoke high-spin effects, except for the effective nutation frequencies.

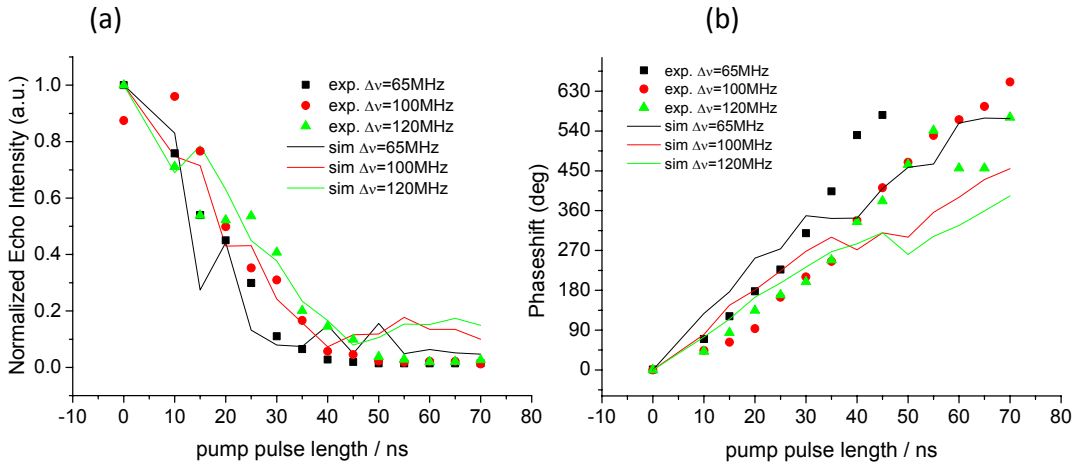

Figure S7. Comparison of experimental versus calculated echo intensities (a) and phase shifts (b) as a function of pump pulse length for three Δν values.

References

1. H. Yagi, D. Banerjee, B. Graham, T. Huber, D. Goldfarb, and G. Otting, *J. Am. Chem. Soc.*, 2011, **133**, 10418-10421.
2. A. Potapov, H. Yagi, T. Huber, S. Jergic, N. E. Dixon, G. Otting, and D. Goldfarb, *J. Am. Chem. Soc.*, 2010, **132**, 9040-9048.
3. X.-C. Su, K. Ozawa, R. Qi, S. G. Vasudevan, S. P. Lim, and G. Otting, *PLoS Negl Trop Dis*, 2009, **3**, e561.
4. I. Gromov, V. Krymov, P. Manikandan, D. Arieli, and D. Goldfarb, *J. Magn. Reson.*, 1999, **139**, 8-17.
5. D. Goldfarb, Y. Lipkin, A. Potapov, Y. Gorodetsky, B. Epel, A. M. Raitsimring, M. Radoul, and I. Kaminker, *J. Magn. Reson.*, 2008, **194**, 8-15.
6. M. Pannier, S. Veit, A. Godt, G. Jeschke, and H. W. Spiess, *J. Magn. Reson.*, 2000, **142**, 331-340.
7. G. Jeschke, V. Chechik, P. Ionita, A. Godt, H. Zimmermann, J. Banham, C. R. Timmel, D. Hilger, and H. Jung, *Appl. Magn. Reson.*, 2006, **30**, 473–498.
8. A. D. Milov, K. M. Salikhov, and M. D. Shirov, *Fiz. Tverd. Tela*, 1981, **23**, 975-982.
9. A. D. Milov, A. B. Ponomarev, and Y. D. Tsvetkov, *Chem. phys. lett.*, 1984, **110**, 67-72.
10. M. K. Bowman and A. G. Maryasov, *J. Magn. Reson.*, 2007, **185**, 270-282.